Deep Learning with Crested Porcupine Optimizer for Detection and Classification of Paddy Leaf Diseases for Sustainable Agriculture

[1] Hussain A and [2] Balaji Srikaanth P
[1,2] Department of Networking and Communications, College of Engineering and Technology (CET),
SRM Institute of Science and Technology, Kattankulathur, Tamil Nadu, India.
[1]ha2514@srmist.edu.in, [2]balajis7@srmist.edu.in

Correspondence should be addressed to Balaji Srikaanth P : balajis7@srmist.edu.in

Article Info
Journal of Machine and Computing (http://anapub.co.ke/journals/jmc/jmc.html)
Doi : https://doi.org/10.53759/7669/jmc202404095
Received 30 March 2024; Revised from 25 May 2024; Accepted 29 July 2024.
Available online 05 October 2024.

Abstract – India has a vast number of inhabitants and the main food source distribution is from agriculture. Agricultural lands are being demolished generally owing to plant and crop illnesses. The detection of plant diseases by using image processing models can aid agriculturalists in defending the farming area from damaging or affecting it. Paddy is the main harvest worldwide. Early recognition of the paddy diseases at dissimilar phases of development is very vital in paddy production. However, the present manual technique in identifying and classifying paddy diseases needs a very educated farmer and is time-consuming. Deep learning (DL) is an effectual research area in the classification of agriculture patterns where it can efficiently solve the problems of diseases identification. Therefore, the articles focus on the design and expansion of Deep Learning based Crested Porcupine Optimizer for the Detection and Classification of Paddy Leaf Diseases (DLCPO-DCPLD) method for Sustainable Agriculture. The main aim of the DLCPO-DCPLD method use DL method for the recognition and identification of rice plant leaf diseases. To accomplish this, the DLCPO-DCPLD technique performs the image pre-processing using Median Filtering (MF) to recover the excellence of the input frames. Next, the ConvNeXt-L method is applied for extraction of feature vectors from the pre-processed images. Also, the Conditional Variational Autoencoder (CVAE) model is utilized for the automated classification of Paddy Leaf diseases. Eventually, the hyperparameter tuning of the CVAE technique is accomplished by implementing the Crested Porcupine Optimizer (CPO) technique. To safeguard the enhanced predictive results of the DLCPO-DCPLD method, a sequence of experimentations is implemented on the benchmark dataset. The experimental validation of the DLCPO-DCPLD method portrayed a superior accuracy value of 99.12% over existing approaches.

Keywords – Image Preprocessing, Crested Porcupine Optimizer, Feature Extraction, Paddy Leaf Disease, Deep Learning.

I. INTRODUCTION

India is one of the significant agricultural nations and the main meal is rice. Concerning the nation's economy, rice is essential. It provides half of the daily caloric intake for individuals and rice production is extremely vulnerable to crop infections that stance a threat to food suppliers globally [1]. Once a year, it is believed that various viruses and pest plagues cause the paddy fields to be spoiled. Owing to their lack of agricultural experience, the new farmers are incapable of identifying the types of diseases. Common approaches for identifying rice diseases include visual analyses and laboratory testing [2]. The laboratory tests were not as effective later they needed more chemical managers and went long to forecast the disease. Increasing rice intake is predicted to continue with an increasing rate of production [3]. Nevertheless, owing to poor field investigation, disease-related problems normally kill a great portion. Many illnesses often attack rice farmers, producing huge financial losses. In the agriculture field, the major study subject is plant disease recognition [4]. In recent days, classification and recognition of plant illnesses has been a difficult job. To evade losses, the agriculture products' quantity and yield, a significant key is plant disease recognition. As sustainable agriculture, recognition of disease, and health monitoring on plants is highly detrimental [5].

These associated studies of plant disease recognition indicate that the illnesses are the recognizable patterns detected on the plants. The physical procedure requires more handling time, a large work quantity, and knowledge of plant diseases [6]. Therefore accurate, real classification and identification of crop illnesses are developed promising by using techniques of DL, and Machine Learning (ML) successful farming quality and productivity. The latest developments in DL, mainly in the image processing field, have revealed greater latent in the initial classification and identification of plant illnesses [7]. Convolutional Neural Network (CNN) were effective in detecting plant diseases depending on plant leaf images. Compared with conventional models, the DL approach provides various benefits such as speed, high accuracy, and the capacity to handle large data quantities [8]. Effectual plant disease detection is significant to lessen crop losses and safeguarding food safety. Advances in DL presents promising solutions for precise and timely detection of plant diseases, which is crucial for improving agricultural productivity [9]. By enhancing disease detection and classification, more sustainable farming practices can be promoted and better manage plant health. Utilizing state-of-the-art optimization approaches can substantially improve the precision and effectualness of these detection systems [10].

This study concentrates on the design and growth of Deep Learning based Crested Porcupine Optimizer for the Detection and Classification of Paddy Leaf Diseases (DLCPO-DCPLD) model for Sustainable Agriculture. The main intention of the DLCPO-DCPLD technique use the DL method for the recognition and identification of rice plant leaf diseases. To accomplish this, the DLCPO-DCPLD technique performs the image pre-processing using MF to recover the excellence of the input frames. Next, the ConvNeXt-L method is applied for extraction of feature vectors from the pre-processed images. Also, the CVAE model is utilized for the automated classification of Paddy Leaf diseases. Eventually, the hyperparameter tuning of the CVAE technique is accomplished by implementing the CPO technique. To safeguard the enhanced predictive results of the DLCPO-DCPLD approach, a sequence of experimentations is implemented on the benchmark dataset.

II. RELATED WORKS

Ritharson et al. [11] suggest a remedy by utilizing DL and transfer learning methods to precisely classify and identify Paddy Leaf illnesses. A complete dataset containing 5932 self-produced Paddy Leaf images has been collected by the benchmark datasets, which are classified into 9 types despite the level of illness spread over the leaves. These types contain various conditions including severe and mild blight, healthy leaves, severe and mild blast, severe and mild brown spot, and severe and mild tungro. Aggarwal et al. [12] present an effective and suitable method for forecasting illnesses in rice leaves by utilizing many various DL techniques. At first, features are extracted by utilizing pre-trained methods, and then the images of Paddy Leaf illnesses by numerous ensemble learning and ML classifications and equated the results. Rajpoot et al. [13] analyze plant illnesses, which affect rice contains 3 various types of illnesses. In the presented method a VGG16 transfer learning with Faster RCNN deep structure is utilized for extraction of features. Next, the collected features are classified by utilizing the random forest technique. Andrianto et al. [14] describe a DL-based rice disease detection system, which contains ML an application on a smartphone, and a cloud server. The smartphone application tasks to take imageries of rice plant leaves and transmit them to cloud server, and obtain classifier outcomes in the data procedure on the plant illnesses type.

Singh et al. [15] introduce a custom CNN structure for classifying and detecting usual illnesses originate in rice plants by decreasing the amount of parameters related to the system. The presented CNN structure was trained by utilizing a database of 4 kinds of usual rice plant diseases. Furthermore, 1400 on-field images of strong Paddy Leaf image datasets are presented for recognition of illness-free plants. Independent experimentations are performed without and with the presence of the strong leaf image dataset. Mahadevan et al. [16] presented a technique of DSGAN^2 with IAPO for rice plant leaf illness recognition. At first, the author served the input of non-healthy and healthy leaves from the gathered database. Next, to enhance the image quality, an ITNN method was applied. Afterward, it utilizes a Segmentation employing an SMNS method to classify the support-intensive color saturation depend upon the improved image. Khasim et al. [17] suggest a complete synopsis of rice plant illnesses and examine DL methods utilized for their recognition. By estimating the disadvantages and advantages of several systems initiated in the works, the research goal is to detect the most precise way of controlling and detecting rice plant illnesses by utilizing DL methods. The author proposes a recent diagnostic and detection method for rice-lead illnesses, which uses ML techniques.

The existing studies in Paddy Leaf disease detection illustrates various limitations. Several techniques, specifically those employing DL and transfer learning models, demand significant computational resources and extensive data, which can affect scalability and real-time accomplishment. Complex approaches comprising diverse DL techniques or advanced methodologies such as VGG16 and Faster RCNN may attain high costs and need vast datasets, potentially limiting their application to less common diseases. Smartphone and cloud-based outcomes encounter threats with data privacy, latency, and connectivity. Furthermore, while custom CNN techniques aim to mitigate parameters, they may sacrifice accuracy, and approaches focused on image quality and segmentation might face difficulty with several or noisy data. Subsequently, there is a requirement for more effectual and practical outcomes that balance accuracy with computational efficiency, effectually handle several data conditions, and perform robustly in real-world scenarios.

III. THE PROPOSED MODEL

In this study, the DLCPO-DCPLD technique is presented for sustainable agriculture. The main intention of the DLCPO-DCPLD technique is in the effective recognition and identification of rice plant leaf diseases. **Fig 1** represents the complete workflow of DLCPO-DCPLD method.

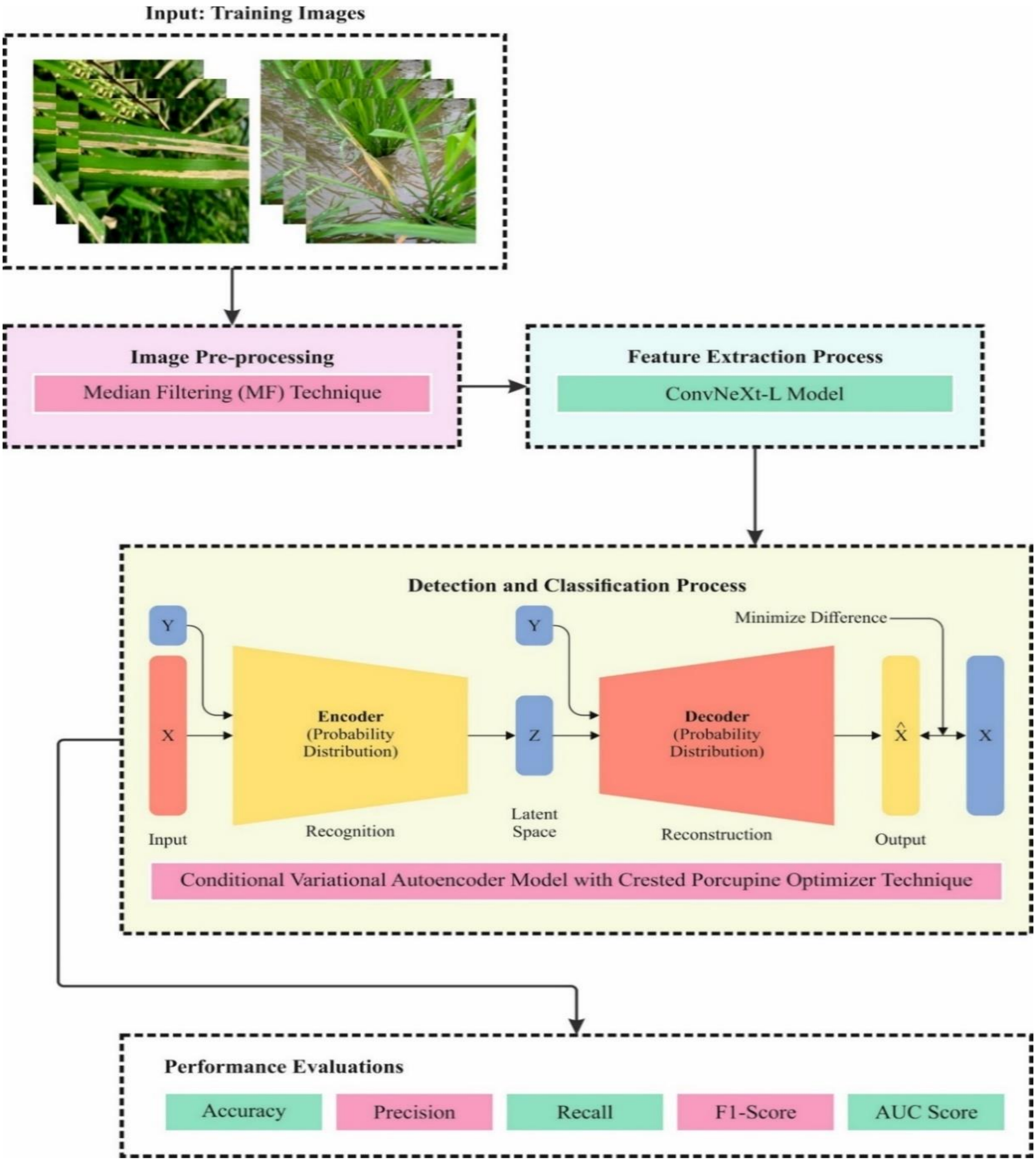

Fig 1. Working Flow of DLCPO-DCPLD Technique.

Image Preprocessing

At first, the DLCPO-DCPLD technique takes place in the image pre-processing using MF to enhance the excellence of the input surrounds. MF is a vital image pre-processing method used in the recognition of rice leaf disease [18]. It functions by substituting every value of pixels with the median value of the strength levels in its zone, efficiently decreasing noise while maintaining edges. This procedure improves the excellence of the leaf images, making disease symptoms more discrete for subsequent analysis. By minimalizing the effect of random noise and unrelated details, MF simplifies more precise classification and identification of numerous Paddy Leaf diseases.

Feature Extraction Using ConvNeXt-L Model

Next, the ConvNeXt-L technique is used to mine feature vectors from the pre-processed images. ConvNeXt depending on the CNN method has been employed for the encoding portion of the suggested network that contains quicker speed of inference and greater accurateness compared with the newly standard transformer-based methods [19]. The creation of the ConvNeXt architecture depends on the new ResNet and is slowly enhanced by a drawing of the Swin Transformer design. Exactly, the ConvNeXt starting point is the ResNet-50 technique. Initially, the ResNet-50 technique was trained with related training technology applied for training vision Transformers and obtained significantly improved outcomes in comparison with the novel ResNet-50 and it is the standard of ConvNeXt. Next, this article examines a sequence of design results, abbreviated as (1) macro design, (2) ResNeXt, (3) reverse bottleneck, (4) large kernel size, and (5) various layered micro designs. **Fig 2** portrays the structure of ConvNeXt-L method.

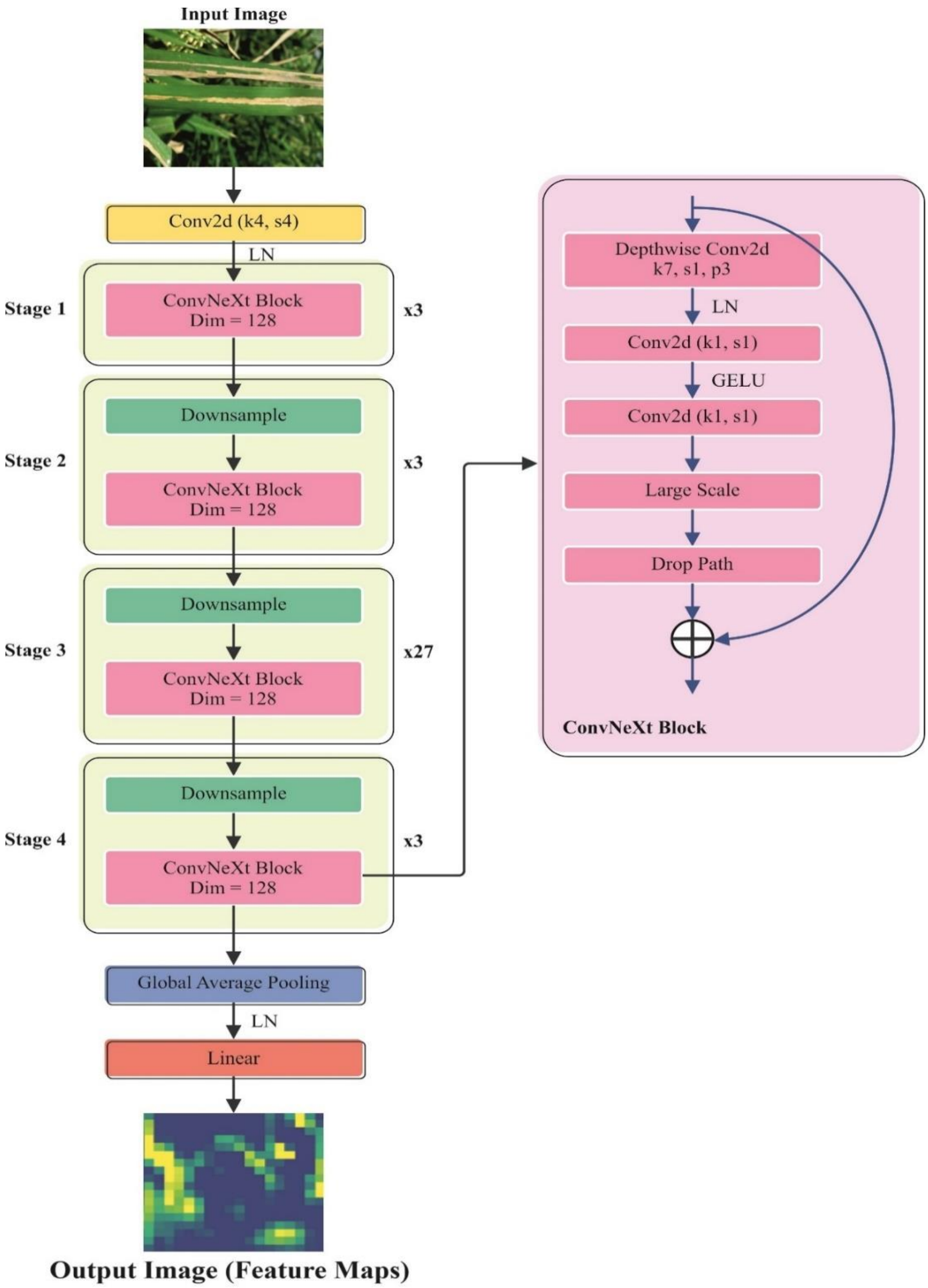

Fig 2. Structure of ConvNeXt-L Model.

Among them, (1) It contains varying the phase computed proportion and stems to 'Patchify'. According to the standard, this article regulates the stacked block numbers in every phase from (3, 4, 6, 3) in ResNet-50 to (3, 3, 9, 3) that adjusts the parameter by Swin-T. In the interim, the ResNet-styled stem cells were changed through a patchy level applied with 4×4, strides four convolutional layers. (2) The ResNeXtify strategy tries to adopt the ResNeXt idea, which employs in-depth conversion and improves the width of the network with similar channel counts as Swin-T (3). The bottleneck blocks in ConvNeXt accept the opposite bottleneck MobileNetV2 unit, which is a structure with a large lower middle and results in efficiently avoiding loss of information. (4) By comparison with the simulated outcomes of various kernel dimensions, the sizes of a convolutional kernel within the ConvNeXt were improved from 3×3 to 7×7. 5. Micro design includes enhancing some particulars, containing substituting ReLU with GELU, smaller amount of normalization and activation functions, replacing Batch Norm (BN) with Layer Normalization (LN), and splitting layer of down-sampling.

When the top design choices, the last ConvNeXt method overtakes the Swin Transformer both inside image detection and classification segmentation responsibilities. Over observation, it is compared to see that ConvNeXt has particular changes in comparison with the other two models. Consequently, a unique backbone network is made with ConvNeXt and rationalized the decoding using the ConvNeXt block of a bottleneck. These methods also strengthen the extraction of feature capacity during the encoder phase to maintain comprehensive content apart from providing the decoder with adequate abilities and features to improve misplaced information of spatial. Further, in comparison with this backbone by other popularised CNN based backbone networks like Vgg-16, Res-Net, and Res2-Net within the new unit, approves the brilliant performance of the recommended model.

The ConvNeXt method, an advanced repetition of the ResNet-50 approach, is obtainable in different types such as ConvNeXt-S, ConvNeXt-T, ConvNeXt-L, ConvNeXt-XL, and ConvNeXt-B. Particularly, this method varies mainly in their structure of network width and depth. The introductory architecture of the ConvNeXt technique includes activation, convolutional, and fully connected layers [20]. Remarkably, ConvNeXt assistances from remaining connections, improving accuracy by effective information propagation through the network. Since there exists a family of ConvNeXt transformers, the ConvNeXtX-L technique is chosen among them. The structure of ConvNeXt-L approach incorporates a 4x4 convolutional layer as well as 36 ConvNeXt Blocks of differing dimensions. Every ConvNeXt Block includes 3 convolutional layers of various sizes, including Layer Scale, Layer Norm, Drop Path components, and GELU activation. For ConvNeXt-L, input images experience resizing and pre-processing to 192x192 sizes.

CVAE Method

Furthermore, the DLCPO-DCPLD technique utilized the CVAE technique for the automated identification of Paddy Leaf illnesses. Depending upon the VAE model, a CVAE is measured as effective to signify the high-dimension joint distributions of aspects [21]. The foremost objective of VAE is the assessment of the relationship among input x_i and the equivalent latent depiction z_i. In the context of VAEs and CVAEs, z_i depicts the latent variable for the i^{th} data instance, capturing its compressed features, which are utilized by the decoder to rebuild the original input. In variational deduction, the later $p(z|x)$ was estimated by a parameterized distribution $q_\theta(z|x)$, which is called variational distribution. The lower limit for $p(x)$ is expressed below in mathematical formulation:

$$L_{\theta,\phi,x} = E_{q_\theta(z|x)}\left[logp_\phi(x|z)\right] - KL(q_\theta(z|x)||p_\phi(z)) \tag{1}$$

The dual vital parts of VAE are encoding $E = q_\theta(x|z)$ and decoding $D = p_{\phi_D}(x|z)$ with parameters θ and ϕ, respectively. They signify functions that map an input x_i to a concealed space z_i and conversely. The re-construction from x_i has been signified by $\hat{x}$. At this time, the signified optimizer is a minimizer of the reconstruction loss below KL divergence as a regularizer. E contains dual outputs μ_i and σ_i, which correspond to the standard deviation and mean of the latent variable z_i. Due to this, the re-parameterization technique is usually employed with $\mu_i + \sigma_i * \varepsilon$ under respect of $\varepsilon_i \sim N(0,1)$ for computing z_i. **Fig 3** illustrates the structure of CVAE model.

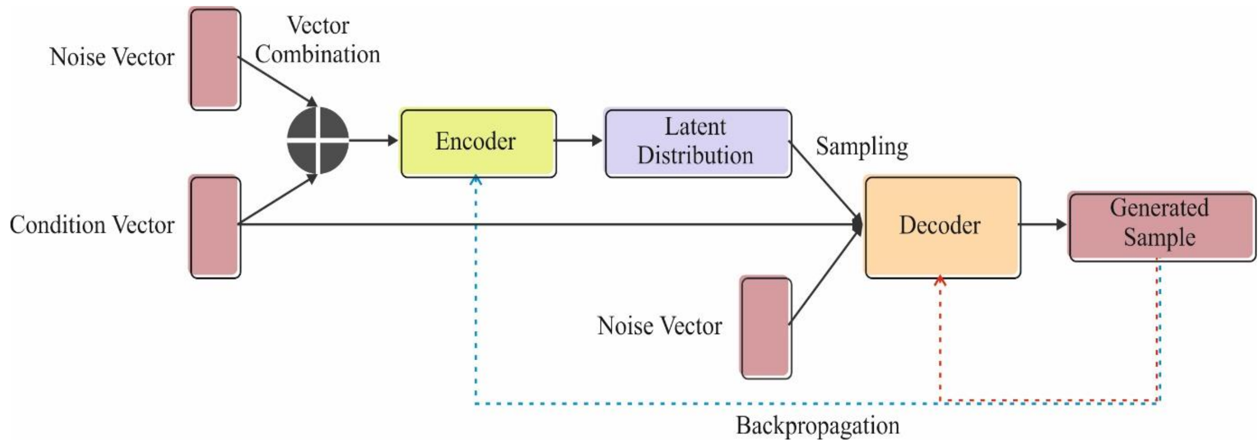

Fig 3. Structure of CVAE Technique.

Contrary to VAE, a CVAE technique depends upon the maximization from the variational lower limit of the restricted probability $p(x|c)$ that aids in making strategies under manifold definite conditions $c = \{c_1 \dots c_n\}$ whereas n denotes the amount of conditions.

$$L_{\theta,\phi,x,c} = E_{q_\theta(z|x,c)}\left[logp_\phi(x|z,c)\right] - KL(q_\theta(z|x,c)||p_\phi(z|c)) \quad (2)$$

The CVAE was functional to rebuild an input x_i below an array of conditions c to contest the outputs of the target $\hat{x}_i$. The foremost part of CVAE E and D are trained by c. It tracks $E = q_\theta(z|x,c)$ and $D = p_{\phi_D}(x|z,c)$ with parameters θ and ϕ, respectively. Its functions were employed to map an input x_i.

CPO-based Hyperparameter Tuning Process

At last, the hyperparameter tuning of CVAE technique is implemented by the design of the CPO technique. CPO model is a new metaheuristic optimizer algorithm that simulates 4 defensive behaviors of crested porcupines such as auditory olfactory, visual, and physical attacks for solving optimizer difficulties [22]. It has robust global searching features and abilities for quick convergence. CPO model, like further metaheuristic swarm techniques, starts the hunting method from a primary group of individuals. As every individual i, a randomly generated location X_i are made inside the search space, formulated mathematically in the following:

$$X_i = L + r \times (U - L)i = 1,2,\cdots,N \quad (3)$$

Here N stands for dimension of population; r represents distributed uniform at randomly generated numbers among 0 and 1; and U and L denotes upper and lower limits, correspondingly. **Fig 4** depicts the architecture of CPO technique.

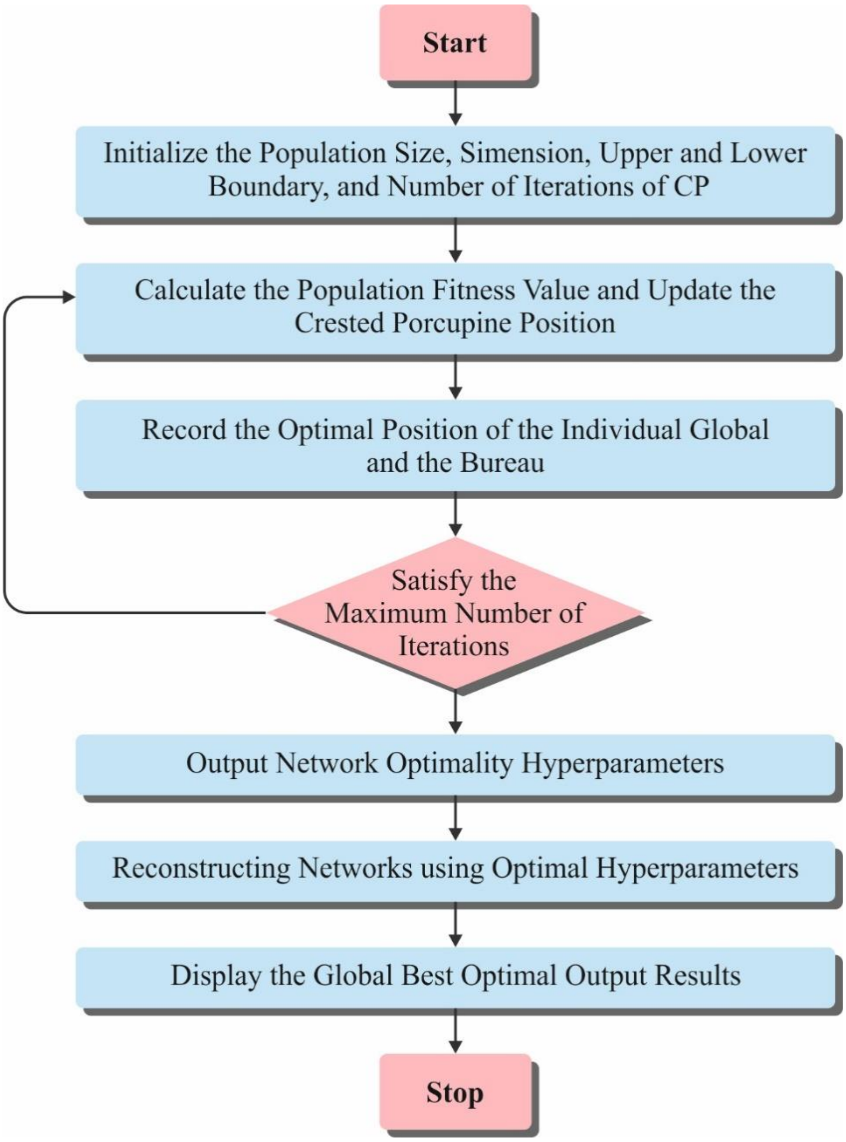

Fig 4. Architecture of CPO Model.

To improve the speed of convergence of an algorithm however preserving population range the Cycle Population Reduction (CPR) method occasionally decreases or increases the dimension of the population based on pre-defined patterns. This mathematically formulated can be

$$N(t) = N_{\min} + (N' - N_{\min}) \times \left(1 - \frac{\mathrm{t}\%T_{\max}}{T_{\max}}\right) \tag{4}$$

Now $N(t)$ signifies the size of the population at present $t\ th$ iteration,· $N_{\min}$ denotes the lowest population dimension; N' symbolizes the primary dimension of the population; $\tau_{\max}$ stands for the highest iteration count for the method; t exists recently generated iteration value; % signifies the modulo process employed to use changes occasionally.

The visual strategy's purpose is to pretend the crested porcupine's behavior after it identifies a predator. In this technique, these imitate the individual's behavior moving near the global finest solution. These mathematic indications are:

$$X_i^{t+1} = X_{CP}^t + \tau_1 \times \left(2 \times \tau_2 \times (X_{CP}^t - y_i^t)\right) \tag{5}$$

whereas X_i^{t+1} signifies i^{th} individual position in the following iteration; X_{CP}^t characterizes the location of a present global finest solution, for example, the location of a top individual placed at present iteration $t; \tau_1$ means randomly generated number depends on a standard distribution, employed to mimic and improve the search ability of the algorithm; τ_2 means randomly formed values in the interval $[0,1]$ utilized to regulate the exploration intensity; $X_{CP}^t - y_i^t$ characterizes the variance among the present global optimum solution and location of present i^{th} individual ; y_i^t symbolizes the mid-point place among i^{th} individual and a randomly selected individual at t^{th} iteration, applied to pretend the predator place.

The sound strategy's intention is to pretend the crested porcupine's behavior producing sounds after predator methods. This algorithm signifies the updating of the position of an individual. The mathematical demonstration is

$$X_i^{t+1} = (1 - U_1) \times X_i^t + U_1 \times \left(y + \tau_3 \times (X_{r1}^t - X_{r2}^t)\right) \tag{6}$$

Where X_i^{t+1} symbolizes i^{th} individual position in the following iteration; X_i^t signifies the i^{th} individual position at present iteration t, U_1 means a randomly formed vector using features set at 0 or 1, applied to mimic whether the CPO produces a frightening sound of the pillager and sound intensities; y characterizes the predator position, typically designed of the places of dual random individuals within the recent population; τ_3 exists randomly generated value inside the interval $[0,1]$ utilized for controlling the stage dimension of the predator's movements; X_{r1}^t and X_{r2}^t symbolize the locations of dual differently chosen random individuals of the population at present t^{th} iterations.

The scent tactic pretends the crested porcupine's discharging behavior is a scent to prevent predators. This technique is signified by updating of individuals to discover novel solutions and evade local goals. In this method, the method can slowly tactic the global optimal while preserving the range of population. The mathematic formulation was mentioned below:

$$X_i^{t+1} = (1 - U_1) \times X_i^t + U_1 \times \left(X_{r_1'} + S_i' \times \left(X_{r_2'} - X_{r_3'}\right)\right) - \tau_3 \times \delta \times \gamma_t \times S_i' \tag{7}$$

whereas X_i^{t+1} signifies i^{th} individual position at the succeeding iteration $t+1$, X_i^t symbolizes ith individual position at the present iteration $t; U_1$ means a randomly formed vector with components set at 0 or 1. Once the value is 1, the individual contributes to the scent approach upgrade; If the range is 0, it doesn't contribute to the scent tactic updates; $X_{r_1'}$ characterizes a random individual position applied to compute the original position; S_i' means scent factor of diffusion employed for controlling the position intensity updating in the scent approach; $X_{r_2'}$ and $X_{r_3'}$ symbolizes the locations of dual other random individuals in the search space, employed together with $X_{r_1'}$ for computing the intensity and direction of the scent diffusion; τ_3 stands for a randomly generated value within the interval $[0,1]$ utilized for controlling the randomness influence in the scent approach; δ denotes a parameter, which manages the search direction, employed to correct the movements route of the individual within the searching space; γ_t means a factor of defense, a time-varying task applied to pretend protective behavior at various points in a period. The mathematic indication can be

$$\gamma_t = 2 \times rand \times \left(1 - \frac{t}{t_{\max}}\right)^{\frac{1}{t_{\max}}} \tag{8}$$

Here $t_{\max}$ represent the maximum iteration counts.

The strategy of physical attack creates defensive behavior, permitting the method for conducting more target-oriented and focused search in the process of search. This approach is mainly proper for the advanced phases of the technique once more advanced searches are required to identify promising parts. The mathematic Eq. expressed below

$$X_i^{t+1} = X_{CP}^t + \alpha \times (1 - \tau_4) \times (X_{CP}^t + X_i^t) + \tau_4 \times F_{CP}^t \tag{9}$$

whereas X_i^{t+1} denotes ith individual position at the following iteration $t+1, X_{CP}^t$ signifies the location of the global optimum solution at the present iteration t, α means convergence force applied for controlling the speed when the model converges to the optimum solution; τ_4 signifies a randomly generated value within the range of [0,1] utilized to present in the physical attack tactic; F_{CP}^t characterizes the average force employed by the global optimum solution X_{CP}^t on predators at the present iteration t. It is calculated depending on the elastic collision principles:

$$F_{CP}^t = \tau_5 \times \alpha_i \times (X_{CP}^t + X_i^t) \tag{10}$$

Now τ_5 signifies another randomly formed integer in the range of [0,1], applied to additionally control the force strength; α_i represent a parameter connected to the location of the i^{th} individual. Algorithm 1 portrays the steps involved in the CPO model.

Algorithm 1: CPO technique
1. Initialize: • Generate a populace of N porcupines with random positions. • Set parameters: number of iterations T, and coefficients for exploration and exploitation (α, β). 2. Evaluate Fitness: • Compute fitness for each porcupine. 3. Find Global Best: • Identify the best fitness value and its corresponding position. 4. Iterate (for t = 1 to T): • Update Positions: $x_i{}^{t+1} = x_i{}^t + \alpha.(G_{best} - x_i{}^t) + \beta.rand.(\mathrm{x}_{i,neigh} - x_i{}^t)$ • Boundary Conditions: o Ensure positions are within feasible space. • Evaluate Fitness: o Compute fitness for updated positions. • Update Global Best: o If any position has better fitness, update global best. 5. Output: • Return the best solution and its fitness value.

The CPO method instigates an Fitness Function (FF) to complete sophisticated classifier efficiency. It expresses a positive numeral to indicate the heightened performance of the candidate solution. In this paper, the minimizer of the classifier rate of error is regarded as the FF and expressed in Eq. (11).

$$\begin{aligned} fitness(x_i) &= ClassifierErrorRate(x_i) \\ &= \frac{no.of\ misclassified\ samples}{Total\ no.of\ samples} \times 100 \end{aligned} \tag{11}$$

IV. PERFORMANCE VALIDATION

In this part, the simulation analysis of the DLCPO-DCPLD method is verified by utilizing the benchmark dataset [23]. The dataset covers 5932 images under four classes as signified in **Table 1**. **Fig 5** represents the sample images of leaf diseases.

Table 1. Details on Dataset

Leaf Disease Name	**No. of Images**
Bacterial leaf blight	1584
Blast	1440
Brown spot	1600
Tungro	1308
Total Images	**5932**

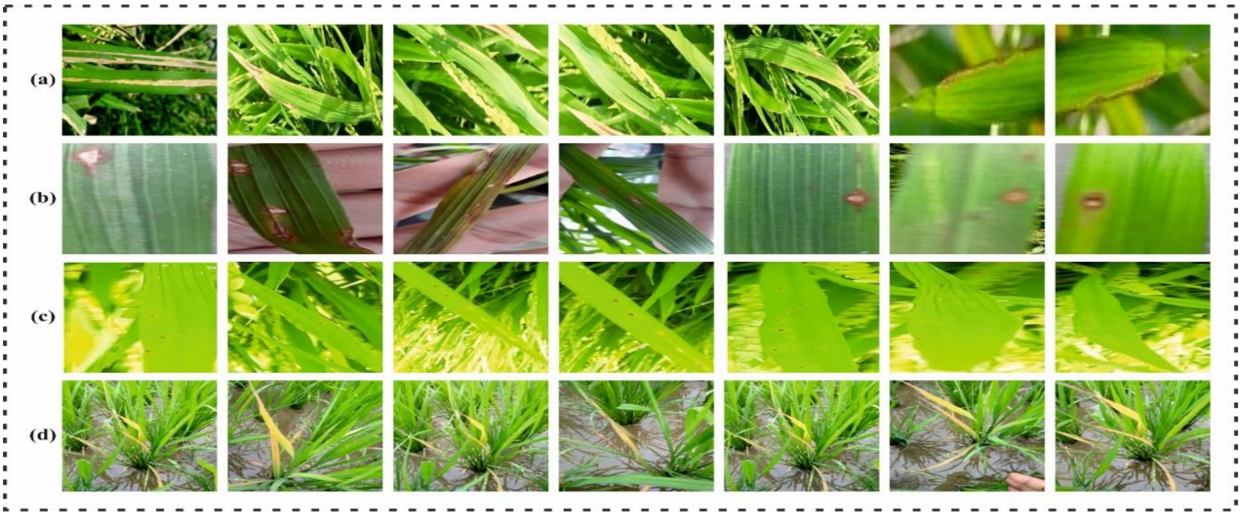

Fig 5. Sample Images of Leaf Diseases.

Fig 6 demonstrates the confusion matrices generated by the DLCPO-DCPLD method below 80%:20% and 70%:30% of Training Phase (TRAP)/Testing Phase (TESP). The results identify that the DLCPO-DCPLD technique has efficient detection and identification of all four classes precisely.

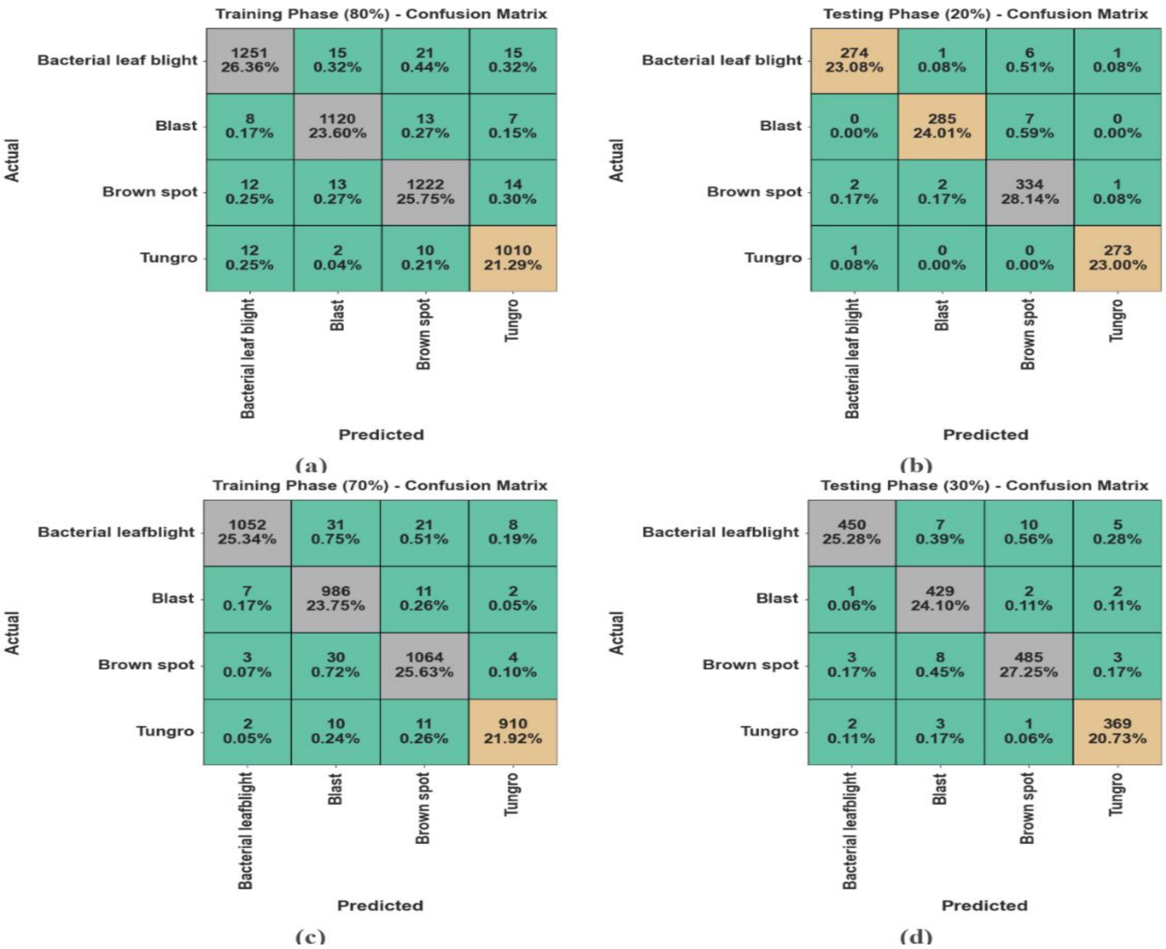

Fig 6. Confusion Matrices of (a-c) 80% and 70% of TRAP and (b-d) 20% and 30% of TESP.

Table 2 and **Fig 7** signify the leaf disease recognition of the DLCPO-DCPLD model on 80%:20% and 70%:30% of TRAP/TESP. The outcomes suggest that the DLCPO-DCPLD method properly recognized the samples. With 80% TRAP, the DLCPO-DCPLD technique attains average $accu_y$, $prec_n$, $reca_l$, $F1_{score}$, and AUC_{score} of 98.50%, 96.99%, 97.06%, 97.02%, and 98.03%, correspondingly. Besides, with 20% TESP, the DLCPO-DCPLD technique gets average $accu_y$, $prec_n$, $reca_l$, $F1_{score}$, and AUC_{score} of 99.12%, 98.35%, 98.23%, 98.28%, and 98.81%, respectively. Moreover, with 70%

TRAP, the DLCPO-DCPLD approach provides average $accu_y$, $prec_n$, $reca_l$, $F1_{score}$, and AUC_{score} of 98.31%, 96.69%, 96.70%, 96.67%, and 97.79%, correspondingly. Also, with 30% TESP, the DLCPO-DCPLD technique attains average $accu_y$, $prec_n$, $reca_l$, $F1_{score}$, and AUC_{score} of 98.68%, 97.35%, 97.45%, 97.39%, and 98.28%, respectively.

Table 2. Leaf Disease Detection Outcome of DLCPO-DCPLD method under 80%:20% and 70%:30% of TRAP/TESP

Classes	$Accu_y$	$Prec_n$	$Reca_l$	$F1_{score}$	AUC_{score}
TRAP (80%)					
Bacterial leaf blight	98.25	97.51	96.08	96.79	97.58
Blast	98.78	97.39	97.56	97.48	98.36
Brown spot	98.25	96.52	96.91	96.72	97.82
Tungro	98.74	96.56	97.68	97.12	98.35
Average	**98.50**	**96.99**	**97.06**	**97.02**	**98.03**
TESP (20%)					
Bacterial leaf blight	99.07	98.92	97.16	98.03	98.42
Blast	99.16	98.96	97.60	98.28	98.63
Brown spot	98.48	96.25	98.53	97.38	98.50
Tungro	99.75	99.27	99.64	99.45	99.71
Average	**99.12**	**98.35**	**98.23**	**98.28**	**98.81**
TRAP (70%)					
Bacterial leaf blight	98.27	98.87	94.60	96.69	97.10
Blast	97.81	93.28	98.01	95.59	97.88
Brown spot	98.07	96.12	96.64	96.38	97.62
Tungro	99.11	98.48	97.53	98.01	98.55
Average	**98.31**	**96.69**	**96.70**	**96.67**	**97.79**
TESP (30%)					
Bacterial leaf blight	98.43	98.68	95.34	96.98	97.44
Blast	98.71	95.97	98.85	97.39	98.76
Brown spot	98.48	97.39	97.19	97.29	98.09
Tungro	99.10	97.36	98.40	97.88	98.84
Average	**98.68**	**97.35**	**97.45**	**97.39**	**98.28**

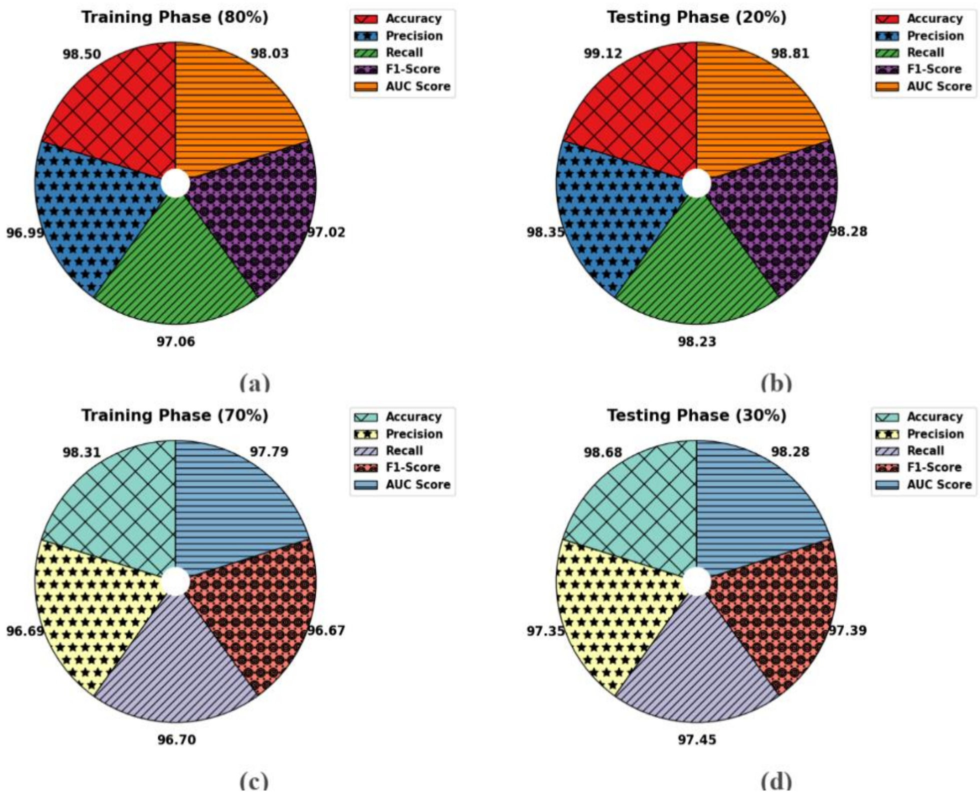

Fig 7. Average of DLCPO-DCPLD Method under 80%:20% and 70%:30% of TRAP/TESP.

Fig 8 demonstrates the classifier results of the DLCPO-DCPLD technique under 80:20 and 70:30. **Figs. 8a-8c** validates the accuracy study of the DLCPO-DCPLD technique. The figure reports that the DLCPO-DCPLD approach extends increasing values over growing epochs. Furthermore, the increasing validation over training exhibits that the DLCPO-DCPLD approach learns competently on the test database. Lastly, **Figs. 8b-8d** validates the loss study of the DLCPO-DCPLD approach. The results specify that the DLCPO-DCPLD technique grasps nearer values of validation and training loss. It is detected that the DLCPO-DCPLD technique learns well on the test database.

Fig 9 determines the classifier results of DLCPO-DCPLD method on 80:20 and 70:30. **Figs. 9a-9c** exposes the PR investigation of the DLCPO-DCPLD method. The results definite that the DLCPO-DCPLD approach outcomes in increasing values of PR. Furthermore, the DLCPO-DCPLD approach can reach greater PR values in every class label. Lastly, **Figs. 9b-9d** explains the ROC study of the DLCPO-DCPLD methodology. The conclusion definite that the DLCPO-DCPLD methodology resulted in enhanced values of ROC. Similarly, the DLCPO-DCPLD methodology can spread boosted values of ROC on every classes.

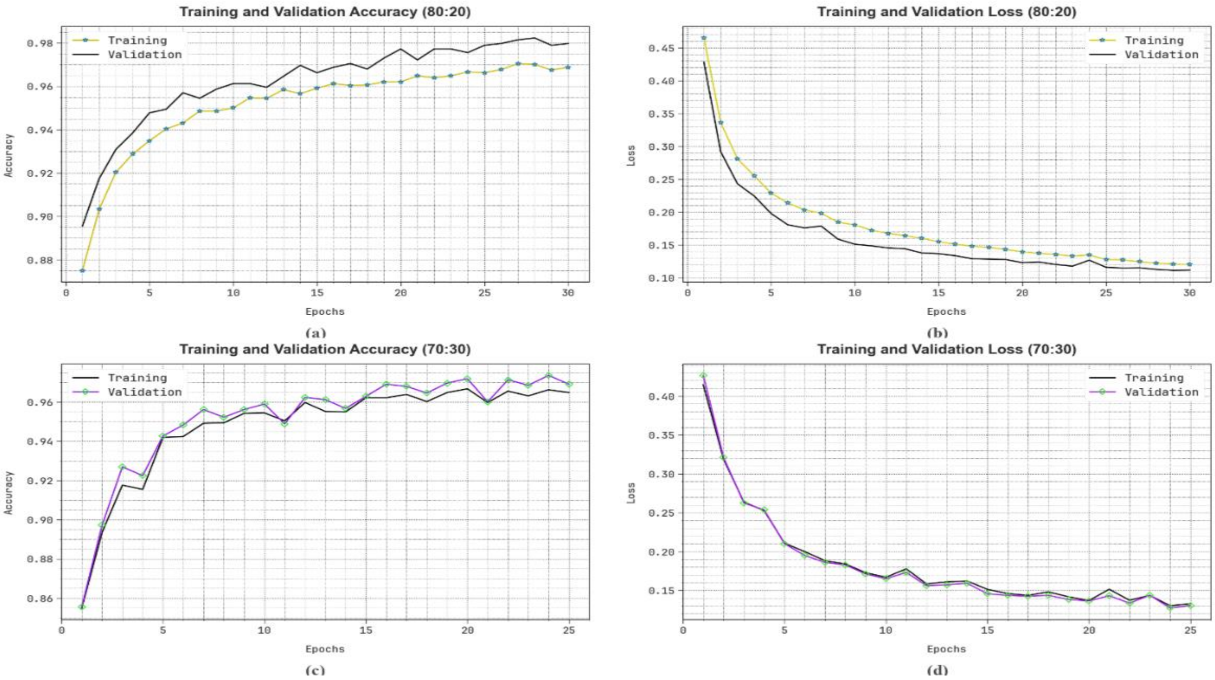

Fig 8. (a-c) Accuracy Curve on 80:20 and 70:30 and (b-d) Loss Curve on 80:20 and 70:30.

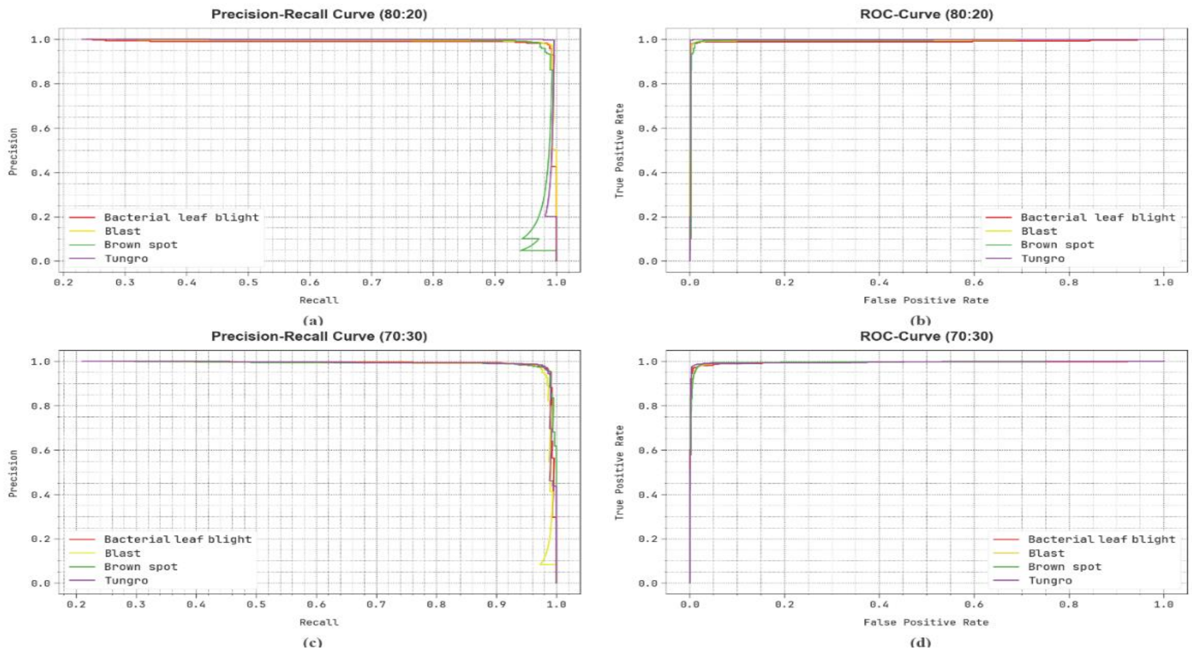

Fig 9. (a-c) PR Curve on 80:20 and 70:30 and (b-d) ROC Curve on 80:20 and 70:30.

Table 3 and **Fig 10** examine the comparison outcomes of the DLCPO-DCPLD technique with the existing methods [24-25]. The outcomes highlighted that the DLCPO-DCPLD model outperformed others with an $accu_y$ of 99.12%, making it the most reliable model for classification tasks. Among them, the PDDIC-DL and FLRLDC-NIIDI models performed very well in terms of precision and recall; therefore, these models would be appropriate for tasks requiring balanced classification. ANN and DAE Classifier returned favorable results that would apply when time on computation is to be saved. Other models, like Xception, DenseNet121, and InceptionResnetV2, performed similarly but with a bit less accuracy overall. Additionally, the DLCPO-DCPLD technique described amended performance with greater $prec_n$, $reca_l$, and $F1_{score}$ of 98.35%, 98.23%, and 98.28%, correspondingly.

Table 3. Comparative Analysis of DLCPO-DCPLD Method with Existing Models [24-26]

Model Names	$Accu_y$	$Prec_n$	$Reca_l$	$F1_{score}$
Xception	93.33	92.55	93.59	94.18
DenseNet121	93.39	93.90	95.57	94.06
InceptionResnetV2	93.44	94.47	94.05	93.62
ANN	94.08	95.26	92.98	94.45
DAE Classifier	94.14	94.63	93.77	94.11
PDDIC-DL	94.95	96.74	96.15	95.27
FLRLDC-NIIDI	95.60	95.23	97.50	96.01
DLCPO-DCPLD	99.12	98.35	98.23	98.28

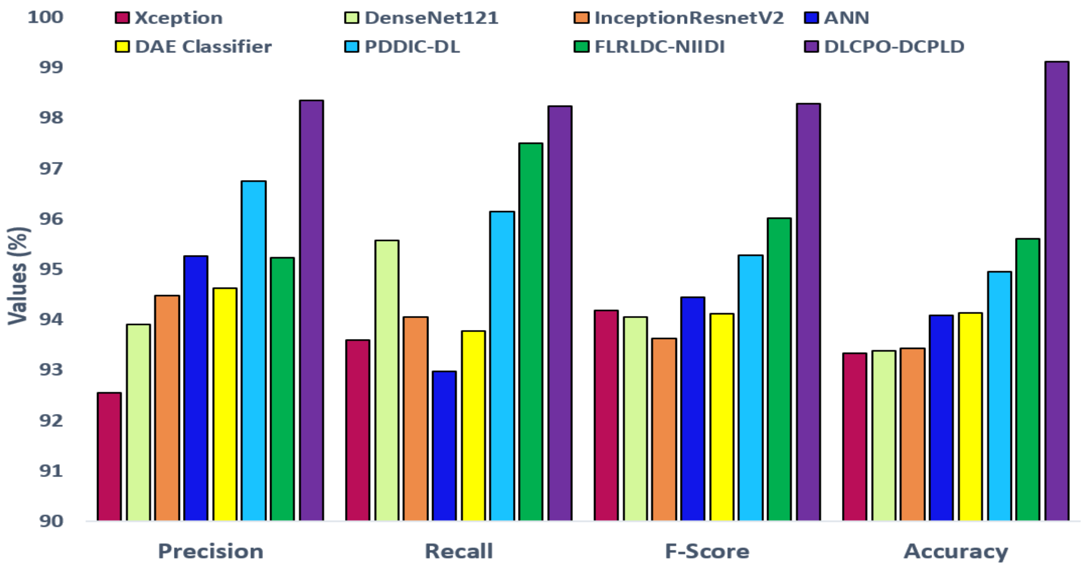

Fig 10. Comparative Analysis of DLCPO-DCPLD Technique with Existing Models.

In **Table 4** and **Fig 11**, the comparative outcomes of the DLCPO-DCPLD technique are shown in terms of Computational Time (CT). The outcomes recommend that the DLCPO-DCPLD approach obtains enhanced performance. Based on CT, the DLCPO-DCPLD approach delivers a lesser CT of 4.38s while the Xception, DenseNet121, InceptionResnetV2, ANN, DAE, and PDDIC-DL models attain superior CT values of 11.91s, 9.18s, 7.66s, 6.94s, 11.16s, 6.85s, and 11.53s, correspondingly.

Table 4. CT Outcome of DLCPO-DCPLD Technique with Recent Models

Model Name	Computational Time (sec)
Xception	11.91
DenseNet121	9.18
InceptionResnetV2	7.66
ANN	6.94
DAE Classifier	11.16
PDDIC-DL	6.85
FLRLDC-NIIDI	11.53
DLCPO-DCPLD	4.38

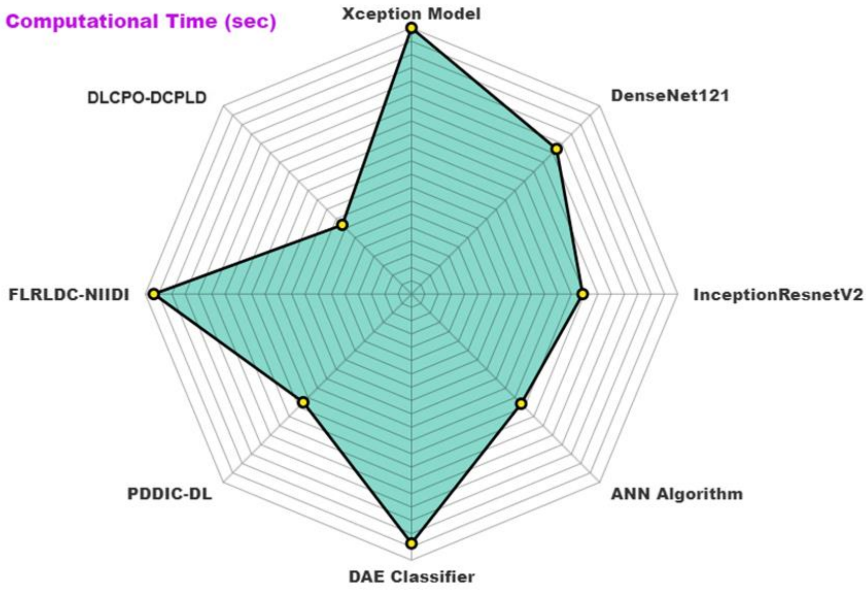

Fig 11. CT Outcome of DLCPO-DCPLD Technique with Recent Methods.

V. CONCLUSION

In this article, a DLCPO-DCPLD method is presented for sustainable agriculture. The main aim of the DLCPO-DCPLD method is to use the DL method for the recognition and classification of rice plant leaf diseases. To achieve this, the DLCPO-DCPLD technique takes place in the image pre-processing using MF to enhance the quality of the input frames. Next, the ConvNeXt-L technique is applied for extraction of feature vectors from the pre-processed images. Besides, the CVAE technique is utilized for the automated classification of Paddy Leaf diseases. Lastly, the hyperparameter tuning of the CVAE technique can be implemented by the design of the CPO technique. To safeguard the enhanced predictive results of the DLCPO-DCPLD method, a sequence of experimentations is implemented on a benchmark dataset. The experimental validation of the DLCPO-DCPLD method portrayed a superior accuracy value of 99.12% over existing approaches. The limitations of the DLCPO-DCPLD method comprises the dependence of the model on MF and may not efficiently handle complex noise patterns or diverse image qualities, potentially affecting the performance of the classification. ConvNeXt-L, while powerful, may need substantial computational resources and may not generalize well across the overall Paddy Leaf disease types. The performance of the CVAE model is heavily dependent on the quality of hyperparameter tuning, and the CPO model might not always converge to the optimal solution, affecting the accuracy of the classification. Future study should concentrate on exploring alternative image pre-processing models, optimizing feature extraction techniques for better scalability, and improving the hyperparameter tuning procedure for enhancing the robustness and generalization of the CVAE model. Furthermore, integrating real-time adaptation abilities and computing the performance of the technique in several environmental conditions could additionally improve its efficiency.

Data Availability

No data was used to support this study.

Conflicts of Interests

The author(s) declare(s) that they have no conflicts of interest.

Funding

No funding agency is associated with this research.

Competing Interests

There are no competing interests

References

[1] L. Y. Win Lwin and A. N. Htwe, “Image Classification for Rice Leaf Disease Using AlexNet Model,” 2023 IEEE Conference on Computer Applications (ICCA), vol. 3, pp. 124–129, Feb. 2023, doi: 10.1109/icca51723.2023.10181847.

[2] B. S. Bari et al., “A real-time approach of diagnosing rice leaf disease using deep learning-based faster R-CNN framework,” PeerJ Computer Science, vol. 7, p. e432, Apr. 2021, doi: 10.7717/peerj-cs.432.

[3] C. Zhou, Y. Zhong, S. Zhou, J. Song, and W. Xiang, “Rice leaf disease identification by residual-distilled transformer,” Engineering Applications of Artificial Intelligence, vol. 121, p. 106020, May 2023, doi: 10.1016/j.engappai.2023.106020.

[4] C. H. Bock, K.-S. Chiang, and E. M. Del Ponte, "Plant disease severity estimated visually: a century of research, best practices, and opportunities for improving methods and practices to maximize accuracy," Tropical Plant Pathology, vol. 47, no. 1, pp. 25–42, Jun. 2021, doi: 10.1007/s40858-021-00439-z.

[5] R. Deng et al., "Automatic Diagnosis of Rice Diseases Using Deep Learning," Frontiers in Plant Science, vol. 12, Aug. 2021, doi: 10.3389/fpls.2021.701038.

[6] S. C. Gopi and H. Kishan Kondaveeti, "Transfer Learning for Rice Leaf Disease Detection," 2023 Third International Conference on Artificial Intelligence and Smart Energy (ICAIS), vol. 7, pp. 509–515, Feb. 2023, doi: 10.1109/icais56108.2023.10073711.

[7] P. Kaur et al., "Recognition of Leaf Disease Using Hybrid Convolutional Neural Network by Applying Feature Reduction," Sensors, vol. 22, no. 2, p. 575, Jan. 2022, doi: 10.3390/s22020575.

[8] V. S. Kumar, M. Jaganathan, A. Viswanathan, M. Umamaheswari, and J. Vignesh, "Rice leaf disease detection based on bidirectional feature attention pyramid network with YOLO v5 model," Environmental Research Communications, vol. 5, no. 6, p. 065014, Jun. 2023, doi: 10.1088/2515-7620/acdece.

[9] S. Sladojevic, M. Arsenovic, A. Anderla, D. Culibrk, and D. Stefanovic, "Deep Neural Networks Based Recognition of Plant Diseases by Leaf Image Classification," Computational Intelligence and Neuroscience, vol. 2016, pp. 1–11, 2016, doi: 10.1155/2016/3289801.

[10] D. I. Patrício and R. Rieder, "Computer vision and artificial intelligence in precision agriculture for grain crops: A systematic review," Computers and Electronics in Agriculture, vol. 153, pp. 69–81, Oct. 2018, doi: 10.1016/j.compag.2018.08.001.

[11] P. I. Ritharson, K. Raimond, X. A. Mary, J. E. Robert, and A. J, "DeepRice: A deep learning and deep feature based classification of Rice leaf disease subtypes," Artificial Intelligence in Agriculture, vol. 11, pp. 34–49, Mar. 2024, doi: 10.1016/j.aiia.2023.11.001.

[12] M. Aggarwal et al., "Pre-Trained Deep Neural Network-Based Features Selection Supported Machine Learning for Rice Leaf Disease Classification," Agriculture, vol. 13, no. 5, p. 936, Apr. 2023, doi: 10.3390/agriculture13050936.

[13] V. Rajpoot, A. Tiwari, and A. S. Jalal, "Automatic early detection of rice leaf diseases using hybrid deep learning and machine learning methods," Multimedia Tools and Applications, vol. 82, no. 23, pp. 36091–36117, Mar. 2023, doi: 10.1007/s11042-023-14969-y.

[14] H. Andrianto, Suhardi, A. Faizal, and F. Armandika, "Smartphone Application for Deep Learning-Based Rice Plant Disease Detection," 2020 International Conference on Information Technology Systems and Innovation (ICITSI), Oct. 2020, doi: 10.1109/icitsi50517.2020.9264942.

[15] S. P. Singh, K. Pritamdas, K. J. Devi, and S. D. Devi, "Custom Convolutional Neural Network for Detection and Classification of Rice Plant Diseases," Procedia Computer Science, vol. 218, pp. 2026–2040, 2023, doi: 10.1016/j.procs.2023.01.179.

[16] K. Mahadevan, A. Punitha, and J. Suresh, "Automatic recognition of Rice Plant leaf diseases detection using deep neural network with improved threshold neural network," e-Prime - Advances in Electrical Engineering, Electronics and Energy, vol. 8, p. 100534, Jun. 2024, doi: 10.1016/j.prime.2024.100534.

[17] S. Khasim, I. S. Rahat, H. Ghosh, K. Shaik, and S. K. Panda, "Using Deep Learning and Machine Learning: Real-Time Discernment and Diagnostics of Rice-Leaf Diseases in Bangladesh," EAI Endorsed Transactions on Internet of Things, vol. 10, Dec. 2023, doi: 10.4108/eetiot.4579.

[18] B. I. Justusson, "Median Filtering: Statistical Properties," Two-Dimensional Digital Signal Prcessing II, pp. 161–196, doi: 10.1007/bfb0057597.

[19] N. Li, X. Yu, and M. Yu, "CMPF-UNet: a ConvNeXt multi-scale pyramid fusion U-shaped network for multi-category segmentation of remote sensing images," Geocarto International, vol. 39, no. 1, Jan. 2024, doi: 10.1080/10106049.2024.2311217.

[20] S. Zhu et al., "Application and visualization study of an intelligence-assisted classification model for common eye diseases using B-mode ultrasound images," Frontiers in Neuroscience, vol. 18, May 2024, doi: 10.3389/fnins.2024.1339075.

[21] S. Eilermann et al., "3D Multi-Criteria Design Generation and Optimization of an Engine Mount for an Unmanned Air Vehicle Using a Conditional Variational Autoencoder," Computer Science Research Notes, 2024, doi: 10.24132/csrn.3401.22.

[22] X. Li et al., "Prediction of Geometric Characteristics of Laser Cladding Layer Based on Least Squares Support Vector Regression and Crested Porcupine Optimization," Micromachines, vol. 15, no. 7, p. 919, Jul. 2024, doi: 10.3390/mi15070919.

[23] Prabira Kumar Sethy, "Rice Leaf Disease Image Samples," Mendeley Data, V1, 2020, doi: 10.17632/fwcj7stb8r.1.

[24] M. Aggarwal, V. Khullar, N. Goyal, A. Alammari, M. A. Albahar, and A. Singh, "Lightweight Federated Learning for Rice Leaf Disease Classification Using Non Independent and Identically Distributed Images," Sustainability, vol. 15, no. 16, p. 12149, Aug. 2023, doi: 10.3390/su151612149.

[25] S. Ramesh and D. Vydeki, "Recognition and classification of paddy leaf diseases using Optimized Deep Neural network with Jaya algorithm," Information Processing in Agriculture, vol. 7, no. 2, pp. 249–260, Jun. 2020, doi: 10.1016/j.inpa.2019.09.002.